# Measurements of Natural Carbonate Rare Earth Elements in Femtogram Quantities by Inductive Coupled Plasma Sector Field Mass Spectrometry

**ARTICLE** *in* ANALYTICAL CHEMISTRY · SEPTEMBER 2011

Impact Factor: 5.64 · DOI: 10.1021/ac201736w · Source: PubMed



**9 AUTHORS**, INCLUDING:

Chuan-Chou Shen
National Taiwan University
**248** PUBLICATIONS **4,717** CITATIONS
SEE PROFILE

Doan Dinh Lam
Vietnam Academy of Science and Technology
**28** PUBLICATIONS **194** CITATIONS
SEE PROFILE

Li Lo
University of Cambridge
**12** PUBLICATIONS **50** CITATIONS
SEE PROFILE

Kuo-Yen Wei
National Taiwan University
**136** PUBLICATIONS **1,249** CITATIONS
SEE PROFILE

analytical chemistry

ARTICLE

pubs.acs.org/ac

# Measurements of Natural Carbonate Rare Earth Elements in Femtogram Quantities by Inductive Coupled Plasma Sector Field Mass Spectrometry

Chuan-Chou Shen,*[,†] Chung-Che Wu,[†] Yi Liu,[‡] Jimin Yu,[§] Ching-Chih Chang,[†] Doan Dinh Lam,[∥] Chien-Ju Chou,[†] Li Lo,[†] and Kuo-Yen Wei[†]

[†]High-Precision Mass Spectrometry and Environment Change Laboratory (HISPEC), Department of Geosciences, National Taiwan University, Taipei, Taiwan 106, R.O.C.

[‡]CAS Key Laboratory of Crust−Mantle Material and Environment, School of Earth and Space Science, University of Science and Technology of China, Hefei, 230026, China

[§]Lamont-Doherty Earth Observatory, Columbia University, Palisades, New York 10964, United States

[∥]Institute of Geological Sciences, Vietnamese Academy of Science and Technology, Vietnam

Supporting Information

**ABSTRACT:** A rapid and precise standard-bracketing method has been developed for measuring femtogram quantity rare earth element (REE) levels in natural carbonate samples by inductively coupled plasma sector field mass spectrometry that does not require chemical separation steps. A desolvation nebulization system was used to effectively reduce polyatomic interference and enhance sensitivity. REE/Ca ratios are calculated directly from the intensities of the ion beams of $^{46}$Ca, $^{139}$La, $^{140}$Ce, $^{141}$Pr, $^{146}$Nd, $^{147}$Sm, $^{153}$Eu, $^{160}$Gd, $^{159}$Tb, $^{163}$Dy, $^{165}$Ho, $^{166}$Er, $^{169}$Tm, $^{172}$Yb, and $^{175}$Lu using external matrix-matched synthetic standards to correct for instrumental ratio drifting and mass discrimination. A routine measurement time of 3 min is typical for one sample containing 20−40 ppm Ca. Replicate measurements made on natural coral and foraminiferal samples with REE/Ca ratios of 2−242 nmol/mol show that external precisions of 1.9−6.5% (2 RSD) can be achieved with only 10−1000 fg of REEs in 10−20 $\mu$g of carbonate. We show that different sources for monthly resolved coral ultratrace REE variability can be distinguished using this method. For natural slow growth-rate carbonate materials, such as sclerosponges, tufa, and speleothems, the high sample throughput, high precision, and high temporal resolution REE records that can be produced with this procedure have the potential to provide valuable time-series records to advance our understanding of paleoclimatic and paleoenvironmental dynamics on different time scales.

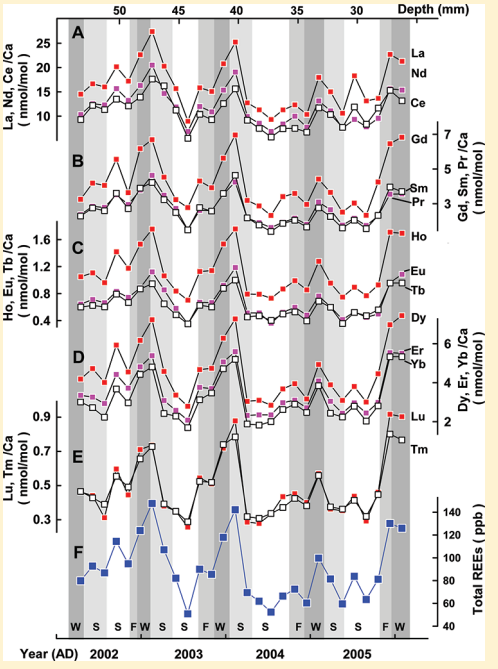


Since the 1980s, rare earth elements (REEs) have emerged as important tracers for diverse applications of the earth sciences, including evolution of lithospheric reservoirs, modern and past environmental changes, and marine geochemistry and ocean circulation.[1−5] Records of REEs in natural carbonate materials, such as corals,[6−9] foraminifera,[10,11] and speleothems,[12,13] have been analyzed for understanding contemporary and late-Quaternary climatic and environmental changes. However, overall applicability has been sharply limited due to the low REE abundances, 1−100s nmol/mol, in most natural samples[6−13] and challenging analytical difficulties.

Different analytical methods, such as neutron activation analysis,[6] inductively coupled plasma atomic emission spectrometry,[14] inductively coupled plasma quadrupole mass spectrometry (ICP−QMS),[15,16] isotope dilution thermal ionization MS (ID−TIMS),[7,10] cathodoluminescence,[17] and laser ablation ICP−MS (LA-ICP−MS),[8,9] have been employed for carbonate REE determinations. ID−TIMS can deliver good precision of 0.1−3% (2 relative standard deviations, 2 RSD); however, labor-intensive sample preparation processes limit the rate of analytical measurements. With improvements in instrumentation, including

**Received:** July 5, 2011
**Accepted:** July 21, 2011
**Published:** July 21, 2011

high sensitivity, low detection limit, and rapid multielement analysis in the past decades, ICP−MS provides the ability to analyze carbonate REEs with a precision of 6−20%.[15,16] For both ID−TIMS and ICP−MS, time-consuming column chromatography is usually required to separate REEs from a matrix, and this step ultimately hinders sample throughput. Simple ICP−MS methods using enriched isotopes and elemental internal standards without chemical separation steps give a 2 RSD of 10−100% for nanomoles per mole level REE analyses.[12,18] Modern LA-ICP−MS methods can offer a direct and fast measurement of micrometer-resolution carbonate REE concentrations;[8,9] however, low REE abundances in corals sharply limit the 2 RSD precision to 26−36% using this procedure.[9]

In this study, we established protocols to directly measure carbonate REE abundances by ICP-sector field (SF)-MS with a 2 RSD reproducibility of 1.9−6.5% for 10−20 μg carbonate samples after their dissolution. We carefully addressed factors affecting the high-precision determination of REE/Ca ratios: (1) spectral interferences,[19,20] (2) mass discrimination and ratio drifting,[21,22] and (3) chemical matrix effects.[21,23] Examples include modern *Porites* corals, planktonic foraminifer *Globorotalia menardii*, and benthic foraminifer *Cibicidoides wuellerstorfi*.

## EXPERIMENTAL SECTION

**Reagents, Standards, and Samples.** Preparation of standards and samples was performed in a class-10 000 geochemical clean room with class-100 benches in the High-Precision Mass Spectrometry and Environment Change Laboratory (HISPEC), National Taiwan University. Water was purified using an ultrapure water tandem system with Millipore Milli-Q Academic and Milli-Q Element. PTFE and polyethylene vials, bottles, and beakers were cleaned by boiling with 3 N guaranteed reagent grade (GR) $HNO_3$ (Merk & CO. Inc.) for at least 4 h. Ultrapure reagents from Seastar or J.T. Baker were used for the chemistry.

One in-house matrix-matched standard, CarbREE-I (REE/Ca ratios of 624−369 nmol/mol, Table S1 of the Supporting Information) was gravimetrically prepared with superpure calcium carbonate powder (purity ≥99.999%, Sigma-Aldrich Inc.) and REE solution standard (La, Ce, Pr, Nd, Sm, Eu, Gd, Tb, Dy, Ho, Er, Tm, Yb, Lu; 10 μg/g, high-purity standards) in 5% ultrapure $HNO_3$. REE/Ca ratios are given in Table S1. One more matrix-matched standard, CarbREE-II with low REE/Ca ratios of 49.4−225 nmol/mol was prepared to evaluate the linearity of intensity signals.

Natural carbonate standards were prepared. Two thousand individuals of a calcitic planktonic foraminifer, *G. menardii* from a marine sediment core ODP1115B (09° 11′ S, 151° 34′ E, water depth 1148.8 m), were cleaned and dissolved to provide a foraminiferal reference solution, FORAM-GM.[22] A 0.5-cm-thick sectioned slab of a modern massive *Porites* coral head ST0506, collected offshore central Vietnam in 2005 (16° 13′ N, 108° 12′ E),[24] was cut along the growth direction.[25] One 0.1-g bulk subsample was cut from the 1991 band, cleaned,[26] and dissolved in 5% $HNO_3$. The foraminifer FORAM-GM and coral ST0506 solutions as well as CarbREE-I were used for assessing analytical reproducibility. Because of the lack of an adequate certified reference material for REE in carbonate samples, an REE-admixed coral standard was applied to validate the proposed procedure. This coral REE standard, CoralM-REE, with theoretical REE/Ca ratios of 33−56 nmol/mol was made by gravimetrically mixing the REE solution standard and one in-house coral standard solution with low REE/Ca ratios of 0.15−5.9 nmol/mol, CoralM, prepared with a modern *Porites* coral collected in Nanwan (21° 57′ N, 120° 45′ E), Taiwan in 2003. It was used for accuracy evaluation.

Coral and foraminiferal samples were also used in this study. Interlaboratory comparison between ICP−QMS[27,28] and our ICP−SF-MS methods was performed by analyzing REE/Ca ratios of a calcitic benthic foraminifer *C. wuellerstorfi* selected from a depth interval of 156−157 cm in a gravity core MW91-9 GGC-15 (0° N, 158° E, water depth 2310 m), located on Ontong Java Plateau. A modern *Porites* coral core, WZI-1, 20 cm in length and 5 cm in diameter, with a growth rate of 7−8 mm/year, was drilled offshore of Weizhou Island (WZI) (21° 01′ N, 109° 04′ E) in the northern SCS in 2009 (Figure S3 of the Supporting Information). Subsamples, 2−4 mg each, were cut on a sliced slab at an interval of 0.7 mm from 2002 to 2005 for monthly resolved REE/Ca determination.

**Safety Considerations.** Nitric acid is a toxic, corrosive reagent that can burn skin and damage respiratory organs. A fume hood with goggles and protective gloves are required to avoid inhalation and contact with skin and eyes. Eye-wash stations and safety showers should be available in case of accidental exposure. Acidic solutions should be neutralized prior to disposal.

**Instrumentation.** Measurements were carried out on a Finnigan Element II ICP−SF-MS (Thermo Electron, Bremen, Germany) at low resolution ($M/\Delta M$ = 300). Radio frequency power was set at 1200 W. Argon flow rates were set at 16 L/min for the plasma gas, 0.8−1.2 L/min for the auxiliary gas, and 0.8−1.0 L/min for the sample gas. An Aridus dry introduction system (CETAC Technologies, NE) with a sample solution uptake rate of 80 μL/min was used. The daily optimum condition was 4−6 L/min for sweep Ar flow and 0.05−0.15 L/min for $N_2$ flow. The temperatures of the spray chamber and desolvator were set at 110 and 160 °C, respectively. This system provided a 5−10-fold enhancement in sensitivity and dramatically reduced the polyatomic inferences from hydrides and oxides.[23] Overall sensitivity was 1.5−2.0 × $10^6$ cps $ppb^{-1}$. The ASX-100 Micro Autosampler (CETAC Technologies, NE) was utilized for automatic sequence measurements.

A single secondary electron multiplier in peak-hopping mode was used to measure the ion beams of $^{46}Ca$, $^{138}Ba$, $^{139}La$, $^{140}Ce$, $^{141}Pr$, $^{146}Nd$, $^{147}Sm$, $^{153}Eu$, $^{159}Tb$, $^{160}Gd$, $^{163}Dy$, $^{165}Ho$, $^{166}Er$, $^{169}Tm$, $^{172}Yb$, and $^{175}Lu$. Ion beam intensities of $^{46}Ca$ and $^{138}Ba$ were measured in analog mode and REEs were measured in ion-counting mode. Cross-calibration between analog and ion-counting modes was performed using a $^{46}Ca^+$ ion beam of 0.8−1.5 × $10^6$ cps before running samples, and instrumental drift was calibrated by measuring bracketed standard solutions between samples. Magnetic-scan (B-scan) mode was used for peak jumping between masses 46, 138, and 159, and electrostatic-scan (E-scan) mode for masses of 139−153 and 159−175. For each measurement, sample solution uptake lasted for 190 s, followed by a 110-s washout step with 5% $HNO_3$. Every four samples were bracketed with one standard. All REE/Ca ratios were calculated directly from ratios of ion beam intensities using external matrix-matched standards to correct for instrumental mass discrimination and ratio drifting. Data were calculated in an off-line data reduction process, modified from Shen et al.[23] All errors given are two standard deviations (2σ) or 2 RSD unless otherwise noted. Detailed instrumental settings and data acquisition methods are summarized in Supporting Information Tables S2 and S3.

## RESULTS AND DISCUSSION

**Blanks and Spectral Interferences.** The procedural blank (PB), including chemical blank and spectral interferences, is

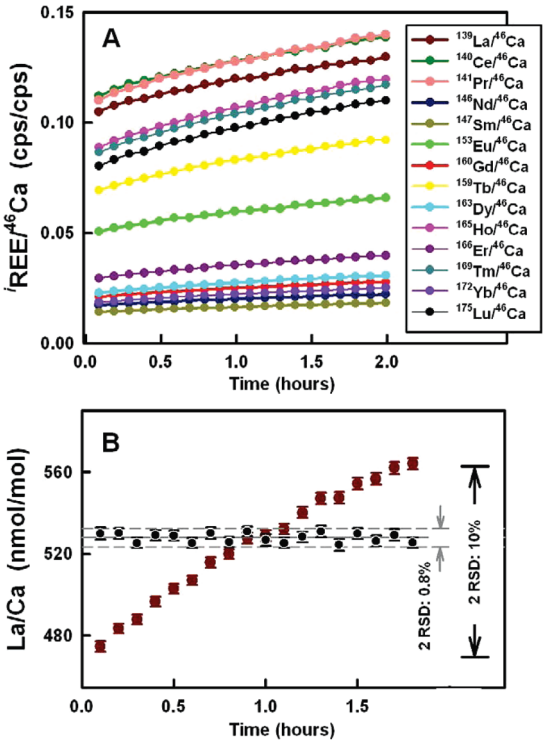


**Figure 1.** (A) Mass drifting in measured REE isotope ($^{i}$REE)/$^{46}$Ca ratios over a 2 h analysis for the 20 ppm Ca CarbREE-I standard solution. (B) Ratio drift in La/Ca over a 2 h measurement experiment. Short-term 2 RSD external precision is improved from ±10% (dark red circles) for the uncorrected values to ±0.8% (black circles) for the standard-bracketing corrected data.

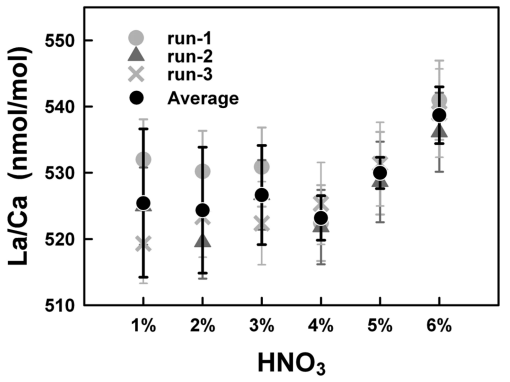


**Figure 2.** Acid effect of $HNO_3$, 1−6%, on La/Ca measurement for the CarbREE-I standard solution with a constant Ca concentration of 20 ppm. Three duplicates are shown in gray symbols with internal errors. The averages are shown in solid circles with 2$\sigma$.

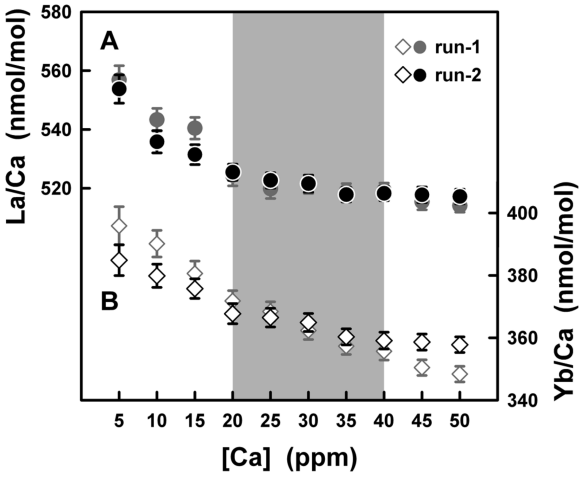


**Figure 3.** Repeat runs for Ca concentration effect on determinations of (A) La/Ca and (B) Yb/Ca. There is a minor [Ca] effect between 20 and 40 ppm (shaded area) (see text).

<2 × $10^3$ cps at 46 atomic mass unit (amu) and <70 cps at 139−175 amu. The PB/signal ratio is 0.1−0.2% for $^{46}$Ca and <0.14% for all REE isotopes of interest in CarbREE-I standard solution with 20−40 ppm Ca. For natural carbonates with <10s nmol/mol REE/Ca, the PB/signal ratio is 2−3% for $^{153}$Eu, $^{159}$Tb, $^{160}$Gd, and $^{163}$Dy, and <1% for other measured REE isotopes. There are two types of instrumental blank in our ICP−SF-MS. One is a residual signal from previous samples. After the uptake of 5% $HNO_3$ for 70 s, the calcium and REE blanks were reduced to <0.02−0.03% of the original signal. These blanks were subtracted from measured ion beams to earn net intensities. Another type of memory interference is a "ghost" ion beam due to a significant contamination after running high concentration calcium samples for 1−2 h. These unexpected abrupt spiky signals were filtered in an off-line data reduction process.

Serious isobaric interference of oxide and hydroxide forms of Ba on Eu was reported for wet introduction systems.[19,20] The BaO/Ba and BaOH/Ba ratios are only 41.9 × $10^{-6}$ and 2.9 × $10^{-6}$, respectively, using the desolvation introduction system (Figure S1). Ba/Ca ratios range from ∼1 to 10 $\mu$mol/mol in marine carbonates of corals and foraminifera.[29,30] The $^{137}$BaO$^+$ signal is <10 cps and the $^{136}$BaOH$^+$ signal is <1 cps at 153 amu. The correspondent isobaric interference for $^{153}$Eu$^+$ is <2.5% for samples with low REE levels of 1−10 nmol/mol. The $^{137}$BaO$^+$ and $^{136}$BaOH$^+$ can cause a high isobaric interference, ∼20% on the $^{153}$Eu$^+$ ion beam, for carbonates with a Ba/Ca level >100 $\mu$mol/mol and Eu/Ca <10 nmol/mol. Hence, we measured the $^{138}$Ba$^+$ ion beam and corrected the isobaric interference using an intensity ratio of 10.7 × $10^{-6}$ [($^{137}$BaO$^+$ + $^{136}$BaOH$^+$)/$^{138}$Ba$^+$] for all carbonates. $^{140}$Ce$^{16}$O$^+$ is an isobaric interference for $^{156}$Gd$^+$ measurement.[31] To avoid this spectral interference, $^{160}$Gd$^+$ was selected to determine Gd content.

**Mass Discrimination and Isotopic Ratio Drifting.** Increased ion transmission with mass causes deviations of measured ratios from true ratios, and this mass discrimination (or mass bias) affects the analytical precision and accuracy of ICP−MS measurements.[21−23] Low-frequency drift of measured isotopic ratios was also observed (Figure 1A), mainly as a result of an analog measure mode used for $^{46}$Ca$^+$ and $^{138}$Ba$^+$, deposition from high-calcium samples, various plasma conditions, and drift in the electronics.[21,22] One typical example of low-frequency drift of measured La/Ca ratios is shown in Figure 1B. La/Ca ratios can vary 20% in 2 h. To correct for these types of biases, the CarbREE-I standard solution was measured after every 4 samples. This allowed for a linear-interpolation correction with a bracketing standard. With the correction, a short-term external 2 RSD precision of 0.8% for La/Ca was achieved (Figure 1B).

**Matrix Effects.** We evaluated the acid effect, which is one type of matrix effect observed in ICP−MS using wet introduction systems with ion beam intensities of different elements.[32,33] As an


dx.doi.org/10.1021/ac201736w |Anal. Chem. 2011, 83, 6842–6848

example, the La/Ca ratios of a 20 ppm-Ca CarbREE-I standard solution in different strengths of $HNO_3$ ranging from 1 to 6% are plotted in Figure 2. The measured La/Ca ratios for 6% $HNO_3$ are slightly higher than the other values, showing a minor acid effect. The external errors of 1.6−2.4% for 1−3% $HNO_3$ are 1.5−2 times larger than the internal errors of 1.1−1.3%, probably related to the formation of nitrate particulates during the desolvation process. The small external errors for high $HNO_3$ levels of 4−5% are comparable to the internal precisions. A compensative 5% $HNO_3$ with good reproducible data was used for routine measurements.

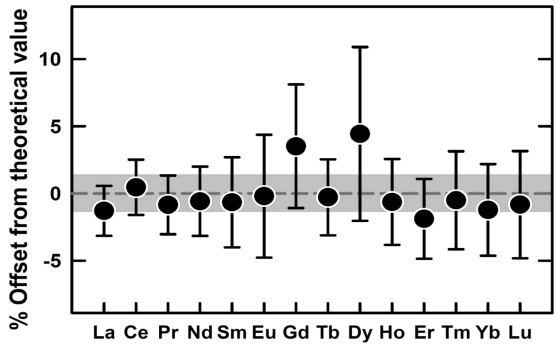


**Figure 4.** Percent offset of measured REE/Ca ratios with long-term 2 RSD error bars (Table S4) from theoretical values in the CoralM-REE standard solution. The shaded area denotes the uncertainty of REE/Ca in the standard.

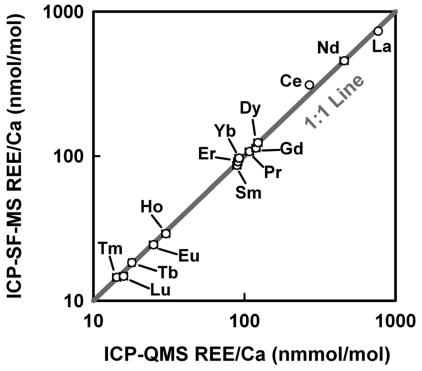


**Figure 5.** Comparison of measured REE/Ca ratios of a benthic foraminifer, *C. wuellerstorfi*, from marine core MW91-9 GGC-15 by our ICP−SF-MS and ICP−QMS[27,28] at the University of Cambridge.

Previous studies[22,34] have shown a matrix effect of Ca concentration on accurate elemental ratio determinations. This effect was addressed by measuring REE/Ca ratios in a range of diluted standard solutions with Ca levels of 5−50 ppm. Figure 3 shows the Ca matrix effect on La/Ca and Yb/Ca. For [Ca] of 5−20 ppm, the measured La/Ca ratio decreases with a slope of ∼17 La/Ca (nmol/mol)/[Ca] (ppm). For [Ca] ≥ 20 ppm, the Ca matrix effect is trivial (Figure 3). A similar Ca matrix effect on Yb/Ca measurement with decreasing trends is observed. A 2−4% change in Yb/Ca between 20 and 40 ppm [Ca] is observed. These observed decreasing REE/Ca trends are likely attributed to space charge effects.[35] REE ions could be strongly defocused within the skimmer with high calcium ion intensities. To attenuate the [Ca] matrix effect, [Ca] in both sample and standard aliquots was adjusted to the same level (within 10%) between 20 and 40 ppm prior to measurement.

One disadvantage for this fast carbonate REE measurement method is inevitable Ca deposition on sampling cones. When running samples with 40 ppm Ca concentration, the intensities of the ion beams decrease by a typical rate of ∼10%/h. The sampling cones should be cleaned manually every day. We suggest analyzing samples with a low Ca concentration of 20 ppm if they have relatively high REE/Ca ratios of tens to hundreds of nanomoles per mole. The daily cleaning step for the sampling cones will not be necessary.

**Accuracy.** REE concentration uncertainties in the commercially available REE solution standard are 1.0%, based on the reports given by High-Purity Standards (Charleston, SC). The use of superpure Sigma-Aldrich calcium carbonate powder contributes 13.6% (±1.4%) for La, 35.5% (±3.0%) for Ce, and

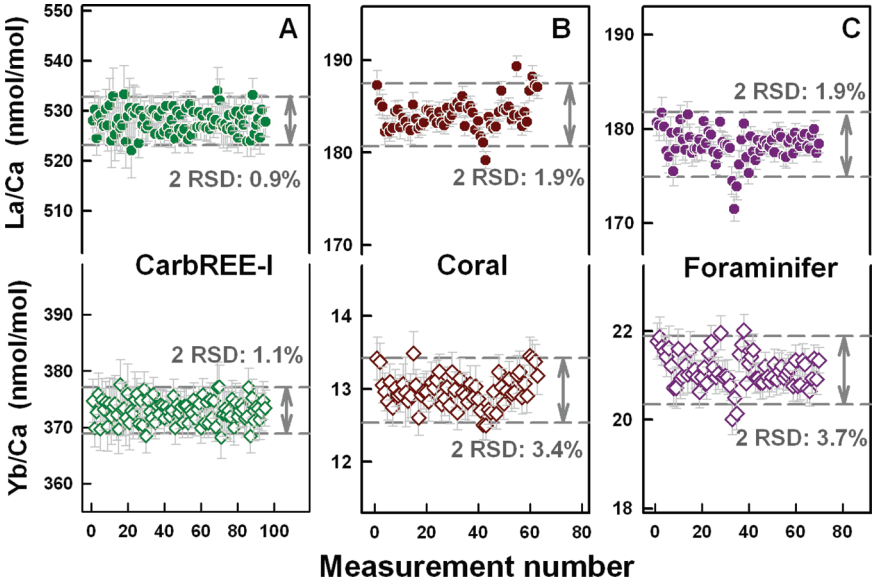


**Figure 6.** Replicate measurements of La/Ca (circles) and Yb/Ca (diamonds) with an internal error of measured REE/Ca ratios in (A) CarbREE-I, (B) coral ST0506, and (C) foraminifer FORAM-GM. External errors are given with a dashed line and values in gray.


dx.doi.org/10.1021/ac201736w |*Anal. Chem.* 2011, 83, 6842–6848

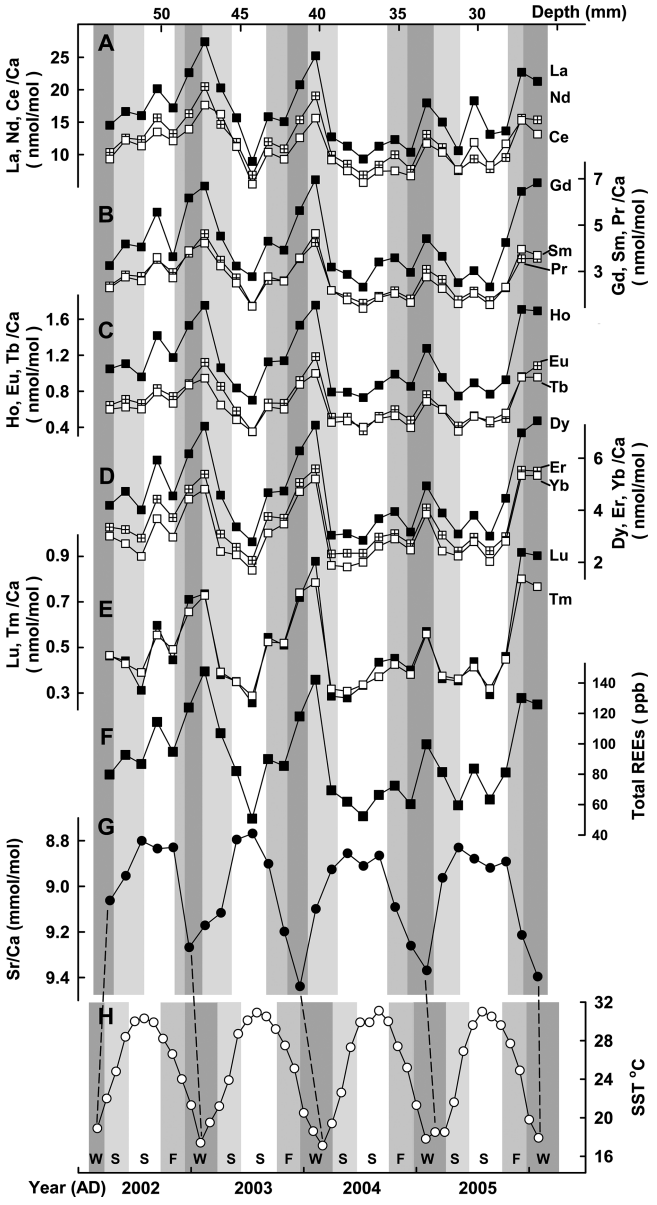


**Figure 7.** Monthly resolved time series for the 4-year period (AD 2002−2005) of (A) La/Ca, Nd/Ca, and Ce/Ca; (B) Gd/Ca, Sm/Ca, and Pr/Ca; (C) Ho/Ca, Eu/Ca, and Tb/Ca; (D) Dy/Ca, Er/Ca, and Yb/Ca; (E) Lu/Ca and Tm/Ca; (F) total REEs; and (G) Sr/Ca[22] for the *Porites* coral, WZI-1, and (H) monthly sea surface temperature (SST) from a WZI meteorological station. Coral REE time series were calendared by aligning coral Sr/Ca maximums with SST minimums. The error bars of REE data are smaller than the symbol size.

<0.3% for all other REEs in the gravimetrically prepared CarbREE-I solution standard. The uncertainties of true REE concentrations in this CarbREE-I standard, including impurities from the calcium carbonate powder, are estimated to be ±1.5% for La, ±3.2% for Ce, and ±1.0% for Pr, Nd, Sm, Eu, Gd, Tb, Dy, Ho, Er, Tm, Yb, and Lu. Measured low CarbREE-II REE/Ca ratios determined with CarbREE-I are insignificantly different from gravimetric values (Table S1), suggesting a good linearity of intensity signals.

The differences between determined REE/Ca ratios and gravimetrically calculated values in the admixed coral standard solution, CoralM-REE, are all less than the long-term uncertainties of 2−6% for coral carbonate (Figure 4). This indicates there is no significant matrix effect to quantify REE contents in natural carbonates by using the in-house standards. An interlaboratory comparison for a benthic foraminifer *C. wuellerstorfi* sample from core GGC-15 shows that our ICP−SF-MS results replicate measurements made by ICP−QMS[27,28] at the University of Cambridge (Figure 5), with the exception of Ce/Ca. This sole discrepancy (13 ± 4% for Ce/Ca) is attributed to slightly heterogeneous Ce contents between the two subsamples that were used in the two laboratories. The above-mentioned experiments indicate our ICP−SF-MS methods can accurately be applied to natural carbonates without a chemistry separation process.

**Precision, and Detection Limit.** Analytical reproducibility over the course of 6 months (Dec 2008−May 2009) determined by repeatedly analyzing the CarbREE-I standard solution is plotted in Figure 6A. Internal 2 RSD precision of REE/Ca ratios ranges from 0.4 to 1.4%. Replicate measurements show that long-term reproducibility ranges from 0.8 to 1.7%, 1.5−2 times that of internal precision. An external uncertainty, for example, is 0.9% for La/Ca and 1.1% for Yb/Ca, respectively (Figure 6A).

Two-month (July−August 2010) REE/Ca data of coral ST0506 (2−242 nmol/mol) and foraminifer FORAM-GM (3−157 nmol/mol) are given in Table S4, and La/Ca and Yb/Ca are also illustrated in Figure 6B,C. Internal 2 RSD precision ranges from 1% to 2% for high (tens to hundres of nanomoles per mol) and low (<10 nmol/mol) REE levels, respectively. External uncertainties of 1.9−6.5% are 2−4 times larger than internal ones.

Large external errors of 5−6% are observed for Eu, Gd, and Dy in coral ST0506 (Table S4). Relatively high 2$\sigma$ external deviations of 5−6% and positive offsets of 3−4% are also observed for Gd and Dy in the reference sample CoralM-REE (Figure 4). The high deviations and offsets are likely caused by polyatomic interferences from trace elements or organic matter or complexes or both, indicating the matrix complexity of natural carbonates.

On the basis of the definition of the detection limit, $3 \times \delta_B$, where $\delta_B$ is the standard deviation of the procedural background of 10−70 cps on ICP−SF-MS, the calculated detection limits of carbonate REE/Ca ratios range from 0.1 to 0.7 nmol/mol. The Eu detection limit varies with Ba content on ICP−MS (see section "Blanks and Spectral Interferences"). The isobaric spectral background should be well-estimated, or the Eu/Ca ratio will be biased.

**Monthly Coral REE Records.** The WZI-1 coral REE diagram shows 4-year monthly averages (AD 2002−2005), normalized to the post-Archean Australian shale (PAAS)[36] and is characterized by heavy REE (HREE) enrichment and a negative Ce anomaly (Figure S2). The two main features resemble those of SCS surface seawater (Figure S2).[37] This observation supports previous suggestions[7,15] that coral REE patterns can reflect ambient seawater conditions.

A striking feature of the monthly resolved REE time series is a clear seasonal cycle, from low levels of 40−80 ppb in summer to high values of 120−140 ppb in winter/early spring (Figure 7). Individual REE/Ca ratios, even as low as 0.3−1 nmol/mol for Eu, Tb, Lu, and Ym, also show coherent seasonal variability, along with total REEs (Figure 7). High coastal seawater REE levels are usually delivered by terrestrial runoff during the rainy season.[8,9] In contrast, the high WZI-1 coral REE levels are observed in the dry winter/early spring season (Figures 7, S3).

WZI, a small island with an area of 25 km$^2$, is isolated from mainland China, well-protected with a dense vegetation cover

and lack of riverine sediment input and local anthropogenic inputs. The most probable source for high REE values is from aeolian dust transported by winter monsoon winds. East Asia is a primary source for natural and anthropogenic dust aerosols in the Northern Hemisphere.[38] The strong and dry winter monsoon not only brings cold air masses but also transports large amounts of dust (average deposition: 2−5 g/m$^2$/year) to eastern and southern China and beyond,[38,39] recorded as high REE levels in WZI corals. This high-resolution coral REE fingerprints could be new proxies for East Asian winter monsoon.

**Summary and Conclusions.** After carefully addressing issues, including spectral interferences, blank and memory effects, ratio drifting and mass discrimination, and matrix effects, a precise procedure for measuring carbonate REEs on ICP−SF-MS has been developed. A high instrumental sample throughput of 8−10 samples/h can be achieved routinely. This high-sensitivity method with good external reproducibility (1.9−6.5%) requires only 10−1000 fg of REEs in 10−20 $\mu$g of carbonate samples.

Compared with labor-intensive TIMS methods,[7,10] only simple cleaning and dissolution steps are involved, and no time-consuming column separation is required in this new procedure. The analytical precision is superior to that of previous ICP−MS[16,18] and LA-ICP−MS methods.[8,9] A clear seasonal cycle of low WZI coral REE/Ca ratios <1 nmol/mol shown by our fast ICP−SF-MS method is difficult to achieve using any other current ICP−MS technique. The examples described here demonstrate the applicability of high-precision monthly coral REEs as proxies for detailed dust history and monsoon evolution. In addition to corals and foraminifera, our method can also be applied to diverse carbonates, such as sclerosponges, tufa, shells, and speleothems. Hence, the carbonate REE-related studies of climate change,[12] environmental research,[8,13] and paleoceanography[11] can benefit from the improvements in precision, sample size, and sample throughput inherent in this new ICP−SF-MS method.

## ■ ASSOCIATED CONTENT

**Supporting Information.** Additional information as noted in the text. This material is available free of charge via the Internet at http://pubs.acs.org.

## ■ AUTHOR INFORMATION

### Corresponding Author

*Phone: 886-2-3365-1917. Fax: 886-2-33665878. E-mail: river@ntu.edu.tw.

## ■ ACKNOWLEDGMENT

We thank H.-W. Chiang, K. Lin, J.-J. Huang, Y.-C. Chou, and C.-Y. Hu for sample collection in the field and laboratory assistance. C.-C.S. greatly appreciates J. A. Dorale and G. S. Burr for constructive suggestions. Comprehensive reviews by three anonymous reviewers significantly improved this paper. This work was funded by ROC NSC grants (98-2116-M002-012, 99-2628-M002-012, and 99-2611-M002-005 to C.C.S. and 97-2627-M002-02 and 98-2627-M002-010 to K.Y.W.) and supported in part by CAS and CNSF grants (XDA05080300, 40830852, 41003002, and 1009 to YL).

## ■ REFERENCES

(1) Elderfield, H.; Greaves, M. J. *Nature* **1982**, *296*, 214–219.
(2) Shaw, H. F.; Wasserburg, G. J. *Geochim. Cosmochim. Acta* **1985**, *49*, 503–518.
(3) Taylor, S. R.; McLennan, S. M. *Rev. Geophys.* **1995**, *33*, 241–265.
(4) Byrne, R. H.; Sholkovitz, E. R. In *Handbook on the Physics and Chemistry of Rare Earths*; Gschneidner, K. A., Jr., Eyring, L., Eds.; 1996, Vol. 23, pp 497−593.
(5) Zhang, J.; Nozaki, Y. *Geochim. Cosmochim. Acta* **1996**, *60*, 4631–4644.
(6) Scherer, M.; Seitz, H. *Chem. Geol.* **1980**, *28*, 279–289.
(7) Sholkovitz, E.; Shen, G. T. *Geochim. Cosmochim. Acta* **1995**, *59*, 2749–2756.
(8) Fallon, S. J.; White, J. C.; McCulloch, M. T. *Geochim. Cosmochim. Acta* **2002**, *66*, 45–62.
(9) Wyndham, T.; McCulloch, M.; Fallon, S.; Alibert, C. *Geochim. Cosmochim. Acta* **2004**, *68*, 2067–2080.
(10) Palmer, M. R. *Earth Planet. Sci. Lett.* **1985**, *73*, 285–298.
(11) Haley, B. A.; Klinkhammer, G. P.; Mix, A. C. *Earth Planet. Sci. Lett.* **2005**, *239*, 79–97.
(12) Zhou, H.; Wang, Q.; Zhao, J.; Zheng, L.; Guan, H.; Feng, Y.; Greig, A. *Palaeogeogr. Palaeocl.* **2008**, *270*, 128–138.
(13) Siklósy, Z.; Demény, A.; Vennemann, T. W.; Pilet, S.; Kramers, J.; Leél-Össsy, S.; Bondár, M.; Shen, C.-C.; Hegner, E. *Rapid Commun. Mass Spectrom.* **2009**, *23*, 801–808.
(14) Kawabe, I.; Kitahara, Y.; Naito, K. *Geochem. J.* **1991**, *25*, 31–44.
(15) Webb, G. E.; Kamber, B. S. *Geochim. Cosmochim. Acta* **2000**, *64*, 1557–1565.
(16) Akagi, T.; Hashimoto, Y.; Fu, F.-F.; Tsuno, H.; Tao, H.; Nakano, Y. *Geochim. Cosmochim. Acta* **2004**, *68*, 2265–2273.
(17) Richter, D. K.; Götte, T.; Niggemann, S.; Wurthet, G. *Holocene* **2004**, *14*, 759–767.
(18) Eggins, S. M.; Woodhead, J. D.; Kinsley, L. P. J.; Mortimer, G. E.; Sylvester, P.; McCulloch, M. T.; Hergt, J. M.; Handler, M. R. *Chem. Geol.* **1997**, *134*, 311–326.
(19) Jarvis, K. E.; Gray, A. L.; McMurdy, E. *J. Anal. At. Spectrom.* **1989**, *4*, 743–747.
(20) Raut, N. M.; Huang, L.-S.; Lin, K.-C.; Aggarwal, S. K. *Anal. Chim. Acta* **2005**, *530*, 91–103.
(21) Rosenthal, Y.; Field, M. P.; Sherrell, R. M. *Anal. Chem.* **1999**, *71*, 3248–3253.
(22) Shen, C.-C.; Chiu, H.-Y.; Chiang, H.-W.; Chu, M.-F.; Wei, K.-Y.; Steinke, S.; Chen, M.-T.; Lin, Y.-S.; Lo, L. *Chem. Geol.* **2007**, *236*, 339–349.
(23) Shen, C.-C.; Edwards, R. L.; Cheng, H.; Dorale, J. A.; Thomas, R. B.; Moran, S. B.; Weinstein, S. E.; Hirschmann, M. *Chem. Geol.* **2002**, *185*, 165–178.
(24) Shen, C.-C.; Li, K.-S.; Sieh, K.; Natawidjaja, D.; Cheng, H.; Wang, X.; Edwards, R. L.; Lam, D. D.; Hsieh, Y.-T.; Fan, T.-Y.; Meltzner, A. J.; Taylor, F. W.; Quinn, T. M.; Chiang, H.-W.; Kilbourne, K. H. *Geochim. Cosmochim. Acta* **2008**, *72*, 4201–4223.
(25) Shen, C.-C.; Lee, T.; Chen, C.-Y.; Wang, C.-H.; Dai, C.-F. *Geochim. Cosmochim. Acta* **1996**, *60*, 3849–3858.
(26) Shen, C.-C.; Hastings, D. W.; Lee, T.; Chiu, C.-H.; Lee, M.-Y.; Wei, K.-Y.; Edwards, R. L. *Earth Planet. Sci. Lett.* **2001**, *190*, 197–209.
(27) Yu, J. M.; Day, J.; Greaves, M.; Elderfield, H. *Geochem. Geophys. Geosyst.* **2005**, *6*, Q08P01; DOI:10.1029/2005GC000964.
(28) Roberts, N. L.; Piotrowski, A. M.; McManus, J. F.; Keigwin, L. D. *Science* **2010**, *327*, 75–78.
(29) Lea, D. W.; Boyle, E. A. *Geochim. Cosmochim. Acta* **1991**, *55*, 3321–3331.
(30) Alibert, C.; Kinsley, L.; Fallon, S. J.; McCulloch, M. T.; Berkelmans, R.; McAllister, F. *Geochim. Cosmochim. Acta* **2003**, *67*, 231–246.
(31) Field, M. P.; Sherrell, R. M. *Anal. Chem.* **1998**, *70*, 4480–4486.
(32) Wollenweber, D.; Strassburg, S.; Wünsch, G. *Fresenius' J. Anal. Chem.* **1999**, *364*, 433–437.
(33) Murphy, K. E.; Long, S. E.; Rearick, M. S.; Ertas., Ö. S. *J. Anal. At. Spectrom.* **2002**, *17*, 469–477.
(34) Green, D. R. H.; Cooper, M. J.; German, C. R.; Wilson, P. A. *Geochem. Geophys. Geosyst.* **2003**, *4*, 8404; DOI:10.1029/2002GC000488.

(35) Gillson, G. R.; Douglas, D. J.; Fulford, J. E.; Halligan, K. W.; Tanner, S. D. *Anal. Chem.* **1988**, *60*, 1472–1474.
(36) McLennan, S. M. In *Geochemistry and Mineralogy of Rare Earth Elements*; Lipin, B. R., McKay, G. A., Eds.; Reviews Mineralogy; Mineralogical Society of America: Washington, DC, 1989, Vol. 21, pp 169−200.
(37) Nozaki, Y.; Lerche, D.; Alibo, D. S.; Snidvongs, A. *Geochim. Cosmochim. Acta* **2000**, *64*, 3983–3994.
(38) Zhang, X. Y.; Arimoto, R.; An, Z. S. *J. Geophys. Res.* **1997**, *102*, 28041–28047.
(39) Jickells, T. D.; An, Z. S.; Andersen, K. K.; Baker, A. R.; Bergametti, G.; Brooks, N.; Cao, J.; Boyd, P. W.; Duce, R. A.; Hunter, K. A.; Kawahata, H.; Kubilay, N.; la Roche, J.; Liss, P. S.; Mahowald, N.; Prospero, J. M.; Ridgwell, A. J.; Tegen, I.; Torres, R. *Science* **2005**, *308*, 67–71.